Corticolimbic structures activation during preparation/execution of respiratory manoeuvres in voluntary olfactory sampling: an intracranial EEG study Authors

Jules Granget, Marie Cécile Niérat, Katia Lehongre, Virginie Lambrecq, Valerio Frazzini, Vincent Navarro, Nathalie Buonviso, Thomas Similowski

▶ **To cite this version:**

Jules Granget, Marie Cécile Niérat, Katia Lehongre, Virginie Lambrecq, Valerio Frazzini, et al.. Corticolimbic structures activation during preparation/execution of respiratory manoeuvres in voluntary olfactory sampling: an intracranial EEG study Authors. 2024. hal-04769884

HAL Id: hal-04769884
https://hal.science/hal-04769884v1

Preprint submitted on 6 Nov 2024

HAL is a multi-disciplinary open access archive for the deposit and dissemination of scientific research documents, whether they are published or not. The documents may come from teaching and research institutions in France or abroad, or from public or private research centers.

L'archive ouverte pluridisciplinaire **HAL**, est destinée au dépôt et à la diffusion de documents scientifiques de niveau recherche, publiés ou non, émanant des établissements d'enseignement et de recherche français ou étrangers, des laboratoires publics ou privés.

Title

Corticolimbic structures activation during preparation/execution of respiratory manoeuvres in voluntary olfactory sampling: an intracranial EEG study

Authors

Jules GRANGET[1,2] Marie Cécile NIÉRAT[1], Katia LEHONGRE[3], Virginie LAMBRECQ[3,4], Valerio FRAZZINI[3,4], Vincent NAVARRO[3,4], Nathalie BUONVISO[5]*, Thomas SIMILOWSKI[1,2]*

* The two last authors contributed equally to the manuscript

Affiliations

1. Sorbonne Université, INSERM, UMRS1158 Neurophysiologie Respiratoire Expérimentale et Clinique, Paris, France

2. AP-HP, Groupe Hospitalier Universitaire APHP-Sorbonne Université, Hôpital Pitié-Salpêtrière, Département R3S, Paris, France

3. Sorbonne Université, Paris Brain Institute, ICM, INSERM, CNRS, Paris, France

4. AP-HP, Pitié-Salpêtrière Hospital, Epilepsy Unit, Reference center of rare epilepsies, ERN-EpiCare, Neurology Department, Paris, France

5. Université Lyon 1, CNRS UMR5292 INSERM U1028, Codage Mémoire Olfaction ,Centre de Recherche en Neurosciences de Lyon, Lyon, France

Corresponding author

Prof. Thomas Similowski, MD, PhD

Department of Respiratory Medicine and Physiology, Intensive Care Medicine, Pulmonary Rehabilitation, and Sleep Medicine

Pitié-Salpêtrière Hospital

47-83 Bd de l'Hôpital, 75651 Paris Cedex 13, France

Telephone: +33 (0) 6 69767252

E-mail: thomas.similowski@sorbonne-universite.fr

Keywords

Olfaction; breathing; respiratory-related brain networks; sniffing; apnoea; intracerebral electroencephalogram; corticolimbic structures.

Running title

iEEG assessment of voluntary olfactory manoeuvres

Abstract

Introduction. Volitional respiratory manoeuvres such as sniffing and apnoea play a key role in the active olfactory exploration of the environment. Their impairment by neurodegenerative processes could thus impair olfactory abilities with the ensuing impact on quality of life.

Research question. Functional brain imaging studies have identified brain networks engaged in sniffing and voluntary apnoea, comprising the primary motor and somatosensory cortices, the insula, the anterior cingulate cortex, and the amygdala. The temporal organisation and the oscillatory activities of these networks are not known.

Methods. To elucidate these aspects, we recorded intracranial electroencephalograms (iEEG) in 6 patients during voluntary sniffs and short apnoeas (12 seconds).

Findings. The preparation phase of both manoeuvres involved increased alpha and theta activity in the posterior insula, amygdala and temporal regions, with a specific preparatory activity in the parahippocampus for the short apnoeas and the hippocampus for sniff. Subsequently, it narrowed to the superior and median temporal areas, immediately after the manoeuvres. During short apnoeas, a particular dynamic was observed, consisting of a rapid decline in alpha and theta activity followed by a slow recovery and increase.

Conclusions. Volitional respiratory manoeuvres involved in olfactory control involve corticolimbic structures in both a preparatory and executive manner. Further studies are needed to determine whether diseases altering deep brain structures can disrupt these mechanisms and if such disruption contributes to the corresponding olfactory deficits.

Key Points

- Both sniff manoeuvres and small apnoeas are associated with oscillatory activity predominantly in low-frequency bands (alpha and theta).
- Preparation of sniff manoeuvres and small apnoeas involve activities in low-frequency bands in the posterior insula and temporal regions that extend to amygdala during both manoeuvres' execution.
- During small apnoeas, activities in low-frequency bands firstly decline before continuously increasing until apnoeas ends.

Abstract figure

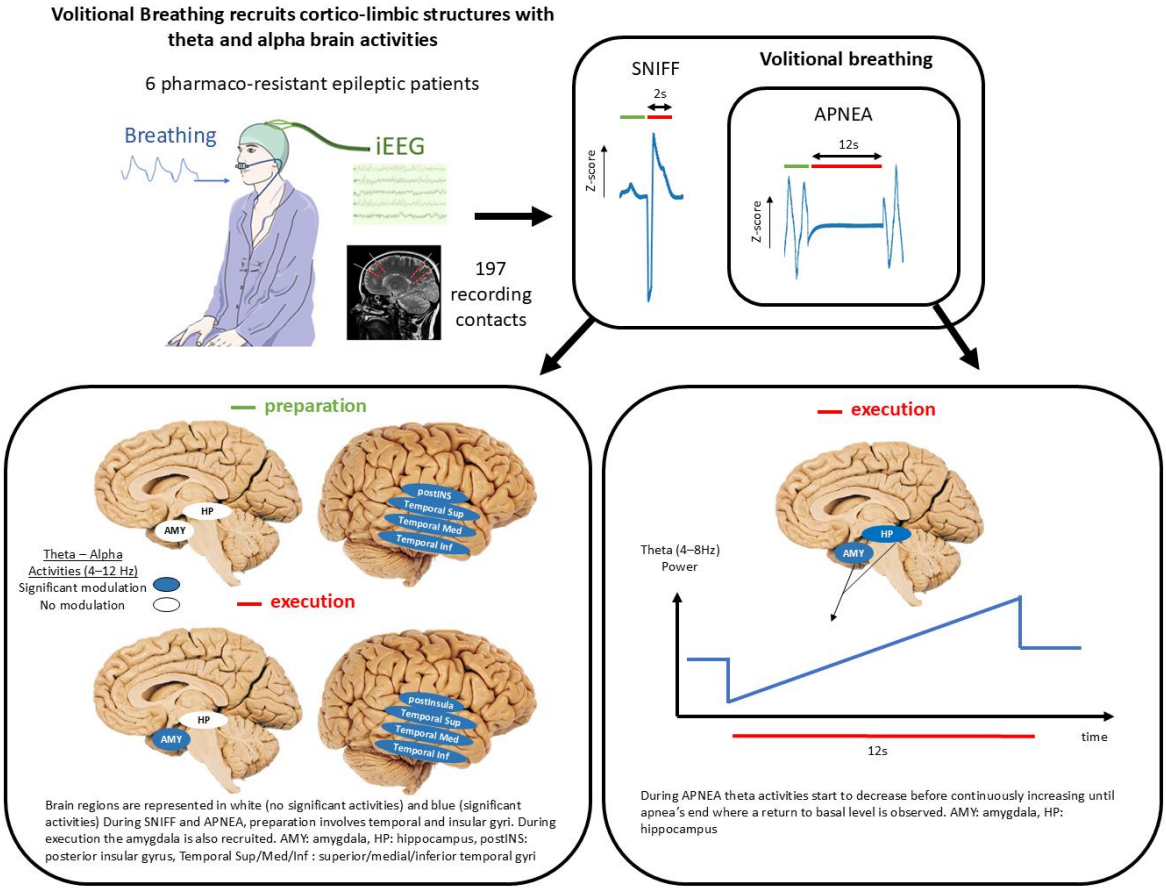

Introduction

Olfaction detects, encodes, and discriminates thousands of odoriferous molecules. It thus plays a key role in environment exploration and control (Roberts et al., 2020; Sharma et al., 2019). It also assigns emotional attributes to perceived odours, which influences mood, memory, and social interactions, hence a crucial contribution to quality of life (Blomkvist and Hofer, 2021; Thomas-Danguin et al., 2014). The olfactory process starts with the binding of odoriferous molecules to sensory neuron receptors in the nasal cavity olfactory epithelium. These molecules travel with the airflow generated by respiratory activity (Yeshurun and Sobel, 2010) that also mobilises the olfactory cilia, a mandatory condition for olfactory perception (Bocca et al., 1965; Grosmaitre et al., 2007). Breathing and olfaction are, therefore, inextricably linked, with breathing automatically providing continuous surveillance of the odoriferous environment (Mainland and Sobel, 2006). On top of that, supra-pontine respiratory-related cortical networks (Herrero et al., 2018; Schottelkotte and Crone, 2022) authorise voluntary manoeuvres such as sniffing –defined as a brief and strong nasal inspiration– and voluntary apnoea –defined as a temporary suspension of breathing activity– that allow volitional olfactory sampling and avoidance, respectively. Diseases deteriorating motor control (e.g. Parkinson's disease or related disorders) could thus impair olfactory abilities with the ensuing negative impact on quality of life.

Functional brain imaging has shown that human sniffing is associated with enhanced activities in the primary motor cortex, somatosensory cortex, premotor area, supplementary motor area, anterior cingulate cortex, insula, amygdala, hypothalamus, and cerebellum (Colebatch et al., 1991; Evans, 2010; Jeran et al., 2013; McKay et al., 2003; Simonyan et al., 2007). Electroencephalographic studies have evidenced that voluntary sniffing follows the general pattern of movement preparation and execution, with premotor (or preinspiratory) potentials preceding motor potentials (Macefield and Gandevia, 1991; Raux et al., 2007). Voluntary apnoea engages a network comprising the dorsolateral prefrontal cortex, globus pallidus, caudate nucleus, insula, parietal cortex, thalamus, and temporal cortex (McKay et al., 2008, 2003). The amygdala may also be involved, as shown by an intracranial electroencephalography (iEEG) study conducted in 6 patients in whom stimulation of the amygdala induced breathing suspension when patients breathed through the nose prior to stimulation (Nobis et al., 2018). These data indicate that the respiratory-related brain networks engaged in sniffing and voluntary apnoea involve structures such as the amygdala, the insula or the anterior cingulate cortex that are implicated in olfactory perception and emotional states (Etkin et al., 2011; Gu et al., 2013; Kulason et al., 2022; Phelps and LeDoux, 2005). However, it is not known how these networks are activated in terms of frequency bands and what temporal dynamics are associated with voluntary sniffing and voluntary apnoea.

In this study, we used intracerebral electrographic recordings (iEEG) to further the understanding of these mechanisms through spatial, temporal, and spectral electrophysiological characterisation. We hypothesised that, despite their markedly different motor characteristics, sniffing and voluntary apnoea would exhibit certain commonalities, notably in brain regions involved in emotional processing such as the amygdala and the insula.

Material and methods

1. Ethical approval

The study conformed to the standards set by the Declaration of Helsinki, except for registration in a database. The procedures were approved by properly constituted ethic committees (INSERM C11-16, C19-55). All patients provided written informed consent prior to enrolment in the study.

2. Setting and patients

The study was conducted between october 2021 and october 2022 within the Epilepsy Unit, Department of Neurology, Pitié-Salpêtrière Hospital, Paris, France, a tertiary university hospital. Adult men and women (aged ≥18 years and free of legal guardianship) who were undergoing presurgical evaluation of pharmaco-resistant focal epilepsy with iEEG implantation were eligible for inclusion. Exclusion criteria were any known significant cardiorespiratory disease likely to interfere with the execution of respiratory tasks or a known susceptibility to epileptic seizures triggered by breathing exercises. Pregnant or lactating women (self-declared) were also excluded. All patients had sufficient command of the French language to fully understand the requirements and aims of the study, and none had cognitive impairment severe enough to prevent them from performing the breathing manoeuvres. Depending on each patient's medical needs, baseline antiseizure medications were either maintained or reduced after implantation. The experimental recordings were performed 3 to 14 days after the implantation of the electrodes. Table 1 presents the characteristics of the patients.

3. Measurements

3.1. iEEG

Each patient had 4 to 13 macroelectrodes implanted (Ad-Tech Medical Instrument Corporation, Wisconsin, USA; 4-12 platinum contacts; 1 mm diameter, 2.4 mm length; 5 mm inter-contact distance; nickel-chromium wiring and polyurethane tubing). The electrode location relied on the suspected seizure onset zone and the trajectories were defined solely based on clinical objectives. Neural activity was recorded using a high-performance amplifier at 4 kHz with a band filter between 0.1 Hz and 1 kHz. (Atlas, Neuralynx®, Inc., Bozeman, MO, USA). For each patient, the least active contact, preferably in the white matter, was selected as the reference electrode.

3.2. Breathing activity

To measure breathing activity in a minimally intrusive manner, we used a nasal pressure cannula connected to a Validyne differential pressure linear transducer from 0 to 140 cm H2O (DP15-32, Validyne, Northridge, CA, USA) for which the output was amplified with a 2000 fold gain preamplifier with a 0.05-500 Hz band-pass filter (Electronique du Mazet, Mazet Saint-Voy, France) before being fed into one of the bipolar inputs of the EEG amplifier. To ensure respiration monitoring in the event of nasal canula failure, breathing was also recorded using a pneumatic-based respiration sensor (Brain Products GmbH, Gilching, Germany).

4. Experimental protocol

4.1. Respiratory tasks

Participants were instructed to breathe in three different ways.

4.1.1. Resting breathing

During resting breathing, patients were instructed to breathe through their nose and to keep their eyes open without focusing on anything specific.

4.1.2. Sniff manoeuvre

Participants were told that "*a sniff consists of a brief and strong inspiration through the nose that starts from the end of expiration*" and the experimenter demonstrated how to perform the manoeuvre. Participants were then asked to perform several sniffs to check their understanding and minimize the impact of learning bias on the subsequent recordings. Then, during the experimental recordings, the patients were instructed to perform repeated self-paced sniffs separated by one or two normal breathing cycles.

4.1.3. Short apnoea (SA)

During SA, patients were instructed to stop breathing at the end of a normal expiration (no pre-apnoea deep breath). They were asked to raise a finger to signal the start of the manoeuvre to the experimenter, who then activated a timer and signalled back to the patients after 12 seconds. The 12-second duration was chosen to capture "passive apnoea", namely the phase of voluntary breath holding that is associated with inhibitory corticobulbar inputs and precedes the subsequent active or "struggling" phase (McKay et al., 2008; *Physiology of Breath-Hold Diving and the Ama of Japan*, 1965).

4.2. Experimental sequence

Participants were comfortably seated throughout the experiments and maintained a generally fixed posture. The protocol consisted of the following sequence (Figure 1):

1) 5-minute period of resting breathing (RB condition);

2) 2 successive blocks of 5 minutes with repeated sniffs, with each block separated by a 2-minute break (SNIFF condition);

3) 5-minute period of resting breathing;

4) 3 successive blocks of 5 minutes with repeated 12-second SA, with each block separated by a 2-minute break (SA condition).

The four conditions were studied in the same order in all patients.

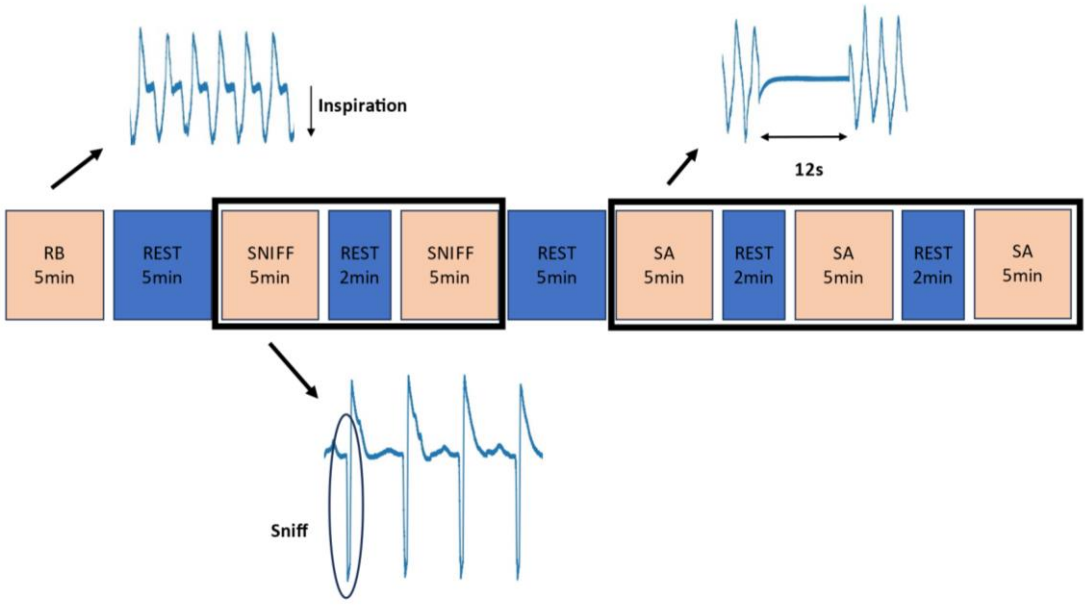

Figure 1. Experimental protocol.
Participants went through the following sequence: 1) resting breathing for 5 minutes; 2) repeated sniffs performed during two 5-minute blocks separated by a 2-minute rest (SNIFF condition); 3) resting breathing for 5 minutes; 4) repeated 12-second short apnoeas (SAs) performed during three 5-minute blocks separated by 2-minute rests. The four conditions were studied in the same order in all patients.

5. Data analysis

5.1. Breathing signal analysis

The detection of respiratory cycles for the resting breathing condition was achieved using an in-house toolbox (Ghibaudo et al., 2023). This algorithm performs 3 main operations: signal smoothing for noise reduction, detection of inspiration/expiration using slope analysis, and exclusion of respiratory cycles with abnormal shapes. Instantaneous respiratory frequency was determined as the inverse of the total breathing cycle duration. Sniffs and SAs were identified visually. For sniffs, start markers were positioned at the onset of the negative inflection of the pressure signal. For SA, start markers were positioned at the peak of inspiration or expiration of the cycle preceding apnoea, and stop markers were positioned 12 seconds after the start.

5.2. iEEG analysis

5.2.1. Electrodes localisation

The spatial localisation of each electrode was determined with the Epiloc toolbox (Pérez-García et al., 2015) developed by the STIM engineering platform in the Paris Brain Institute (https://icm-institute.org/en/cenir-stim) using co-registered pre-implantation 1.5 T or 3 T MRI scans and post-implantation CT and MRI scans. Following the normalisation of MRI-pre, MRI-post and CT-post into the Montreal Neurological Institute space, contact localisation was automatically labelled referring to Desikan-Killiany-Tourville atlas parcellation

(Desikan et al., 2006) in the patient's native space. This process was performed using a Freesurfer image analysis suite (https://surfer.nmr.mgh.harvard.edu/) embedded in the Epiloc toolbox, followed by manual verification and correction, if necessary. Subsequently, all EEG signals were re-referenced to their adjacent neighbour on the same electrode, yielding a bipolar montage. With this approach, bipolar iEEG signals represent the difference in local field potentials between those two points, which does not always reflect the region between the contacts. As is common practice, we used the midpoint between the two contacts as representing the signal. The resulting coordinates were determined as the mean of the MNI coordinates of two adjacent contacts composing the bipole and the corresponding structure was subsequently extracted with the Epiloc toolbox and visually inspected.

5.2.2. Visual signal assessment and contact selection

An initial visual inspection of continuous EEG signals was conducted to remove time segments showing obvious artifacts. Contacts with excessive artifacts or suspected epileptic activities were discarded. Contacts located in the white matter, in ventricles, or outside the brain were also discarded. Of note, the medical team in charge of the patients carefully examined all the retained contacts for localization and signals provided, in order to ensure that none of the contacts used for our analyses were located within epileptic foci.

Of the 383 contacts recorded in total, 172 contacts were rejected and 211 contacts were identified as usable signals (amygdala: 17; fusiform gyrus: 2; hippocampus: 24; posterior insula: 3; lingual: 4; orbito frontal cortex: 1; parahippocampal gyrus:-7; temporal pole: 6; supra marginal: 1; inferior temporal gyrus: 48; medial temporal gyrus: 53; superior temporal gyrus: 42).

5.2.3. Selection of particular regions of interests

From the 211 contacts selected for analysis, we concentrated on a restricted set of seven regions of interest (amygdala, hippocampus, posterior insula gyrus, parahippocampal gyrus, inferior temporal gyrus, medial temporal gyrus, superior temporal gyrus of known significance in both volitional respiratory manoeuvres and emotional cognition (Koritnik et al., 2009; Simonyan et al., 2007) that were consistently recorded across all patients (Figure 2). These seven regions of interest represent 197 contacts.

5.2.4. Pre-processing

After the above initial phase, signal preprocessing consisted in mean centring all data (github.com/JulesGranget/Script_Python_iEEG_Paris_git) and applying a 50 Hz line noise filter (Python MNE toolbox https://doi.org/10.5281/zenodo.592483).

5.2.5. Post-processing

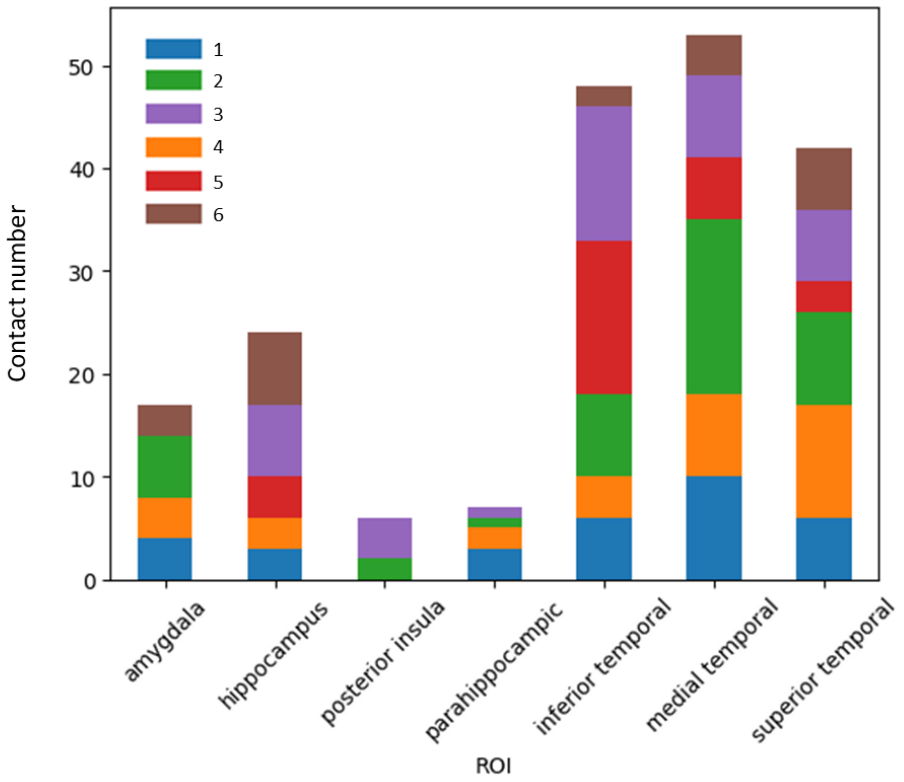

Figure 2. Number of contacts in the analysed regions of interest.
The vertical bars indicate the total number of contacts analysed for each region of interest (ROI), each patient being represented by a specific colour. See "Discussion" for the justification of the ROI selection. Five ROIs (amygdala, hippocampus, inferior temporal, medial temporal, and superior temporal gyri) were recorded in all patients, in variable proportions.

iEEG signals were analysed using a population-wise approach, all contacts from the same anatomical location being pooled together. Data were analysed using Morelet's wavelets (Kronland-Martinet et al., 2012). A total of 150 complex wavelets were manually generated from 2 Hz to 150 Hz with a log-scaled number of cycles from 7 to 41 covering all frequencies. The analysis covered the theta (4-8 Hz), alpha (>8-12 Hz), beta (>12-40 Hz) and gamma (>50-120 Hz) frequency bands, all of which are relevant to human olfactory processing (Jiang et al., 2017; Yang et al., 2022). The iEEG signals were then convolved with these wavelets and power was extracted. The resulting time-frequency maps were normalized across all frequencies on all conditions using the robust z-score (rscore) method or median absolute deviation method, a variation of the z-score method that replaces outlier-sensitive mean and standard deviation by median and median absolute deviation. These frequency maps were then processed differently depending on the condition, as follows. Regarding the resting breathing condition, a phase-based approach was used rather than a time-based approach to capture power modifications throughout the respiratory cycle, thus respecting cycle-by-cycle variability (Kronland-Martinet et al., 2012). Markers were identified for the onset of each inspiration and expiration, and all respiratory cycles were stretched over the same number of time bins. This stretched signal was then convoluted and the resulting time-frequency map were averaged

using their median. Secondly, Regarding the SNIFF and SA conditions, the above precaution was unnecessary as the corresponding respiratory manoeuvres were all time-locked. A time-based approach was, therefore, used to segment the respiratory signal. Selected sniff segments extended from 3 seconds prior to 3 seconds after the sniff. Selected SA segments extended from 12 seconds prior to 12 seconds after its end. This time extraction was selected to match the apnoea duration, constituting a baseline before and after the apnoea. Finally, for any given brain region, a median time frequency map was computed from all patients' time-frequency maps, using the same scale across all conditions. This scale was obtained by generating a distribution of all time frequency values, extracting the 99th percentile of this distribution, and using it as the upper limit of the scale, with its opposite as the lower limit.

To compare the temporal activation of all brain regions during SNIFF and SA, TF maps were segmented according to where visual inspection rendered a statistically significant difference possible. For SNIFF, 4 segments of 1 second were used from 2 seconds prior to 2 seconds after the SNIFF. For SA, 12 segments of 3 seconds were used from 12 seconds prior to 24 seconds after the SA start. For each of these segments, median power was extracted for all patients and then the median was computed across patients for each brain region. These representations are referred to in the statistical analysis part as TF maps matrices.

6. Statistical analysis

6.1. Permutation based statistics

The statistical analysis of time-frequency maps was conducted using a cluster permutation approach to detect significant power increases during SNIFF and SA respective to resting breathing considered as baseline (Maris and Oostenveld, 2007). In any given region, stretched TF maps were extracted from all subjects for resting breathing, baseline, and the condition of interest. A series of 1000 permutations was performed, each consisting of the following steps: first, a shuffled TF map was constructed by a random selection between the baseline and the condition to match the number of cycles originally present in the condition of interest. The median shuffled TF map was computed, and the minimum and maximum were extracted (see above). By repeating this process 1000 times, we were able to build 2 populations for the minimum and maximum. Their median represented the threshold for extracting clusters, every value in the time frequency map tested below the obtained minimum or above the obtained maximum is identified as significant and form a cluster (Figure 3). Clusters were then sorted by size and any above the 99th percentile of the cluster size distribution (alpha=0.01) were considered to be significantly different from the resting breathing condition.

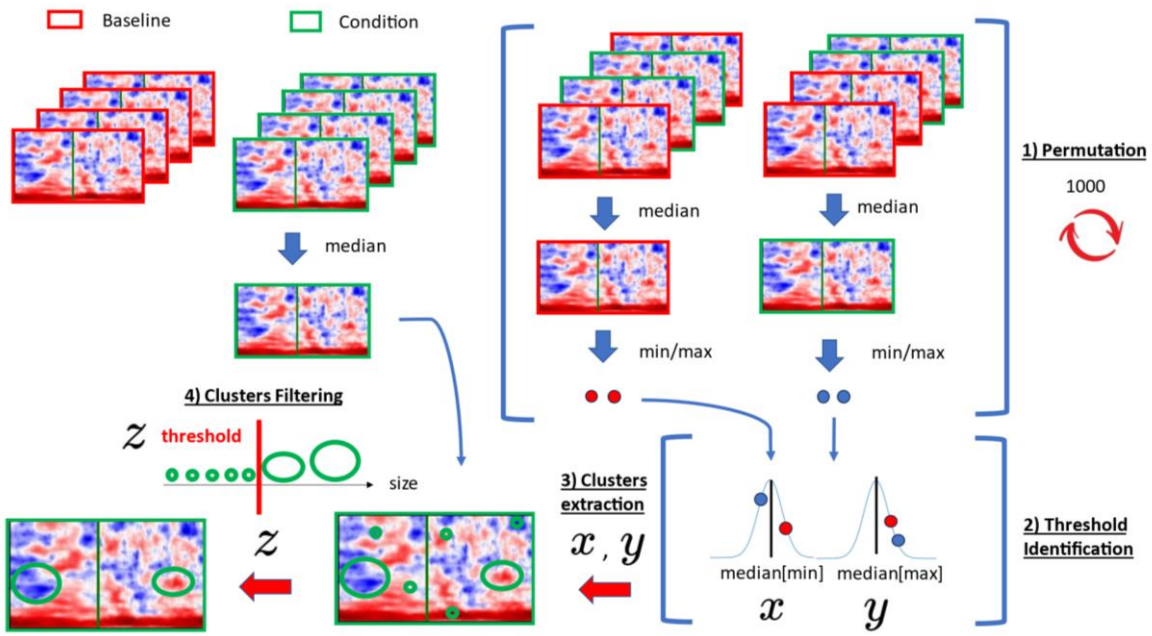

Figure 3. Permutation procedure.
For a given experimental condition, the median of time frequency (TF) maps across observations was computed and compared to a surrogate distribution to indicate significant power modulations according to the following process. 1) all TF maps for our experimental conditions were shuffled with the resting breathing set of TF maps. We computed the median across the shuffled set of TF maps and extracted the minimum and maximum values. 2) Across permutations, we generated two distributions for minimum and maximum values. We then extracted the median for both distributions. 3) With these two thresholds applied to the measured TF map, we revealed clusters. 4) Clusters were then sorted by size, with clusters considered significant when ~~those~~ above the 99th percentile of the cluster size distribution.

As a result, highlighted clusters represent significant power increases or decreases compared to resting breathing (Maris and Oostenveld, 2007).

For TF maps matrices, in each segment, power modifications in a given frequency band were considered significantly different when more than 5% of the TF points fell below the significance threshold during the permutation-based cluster process (see below). To identify concurrent power modifications visually and easily, the results are represented on a time and space matrix.

6.2. Linear mixed models

Visual inspection of the signals during SA suggested dynamic power increases in certain regions of interest. To determine whether these trends were statistically significant, we used linear mixed models to take into account a possible random subject effect. The python package *mixedlm()* function from *statsmodels.formula.api* was used to compute the linear mixed model, with time as fixed effect and patients as random effect. Medians for power were computed for all patients in all frequency bands. Then, assumptions for proper model usage were verified using normality and quartile-to-quartile plot for residuals. After having checked the assumptions, all points between 0 and 12 seconds were included in the model.

Results

1. Breathing pattern

All the patients understood and correctly performed the breathing tasks (Table 2 and Figure 4).

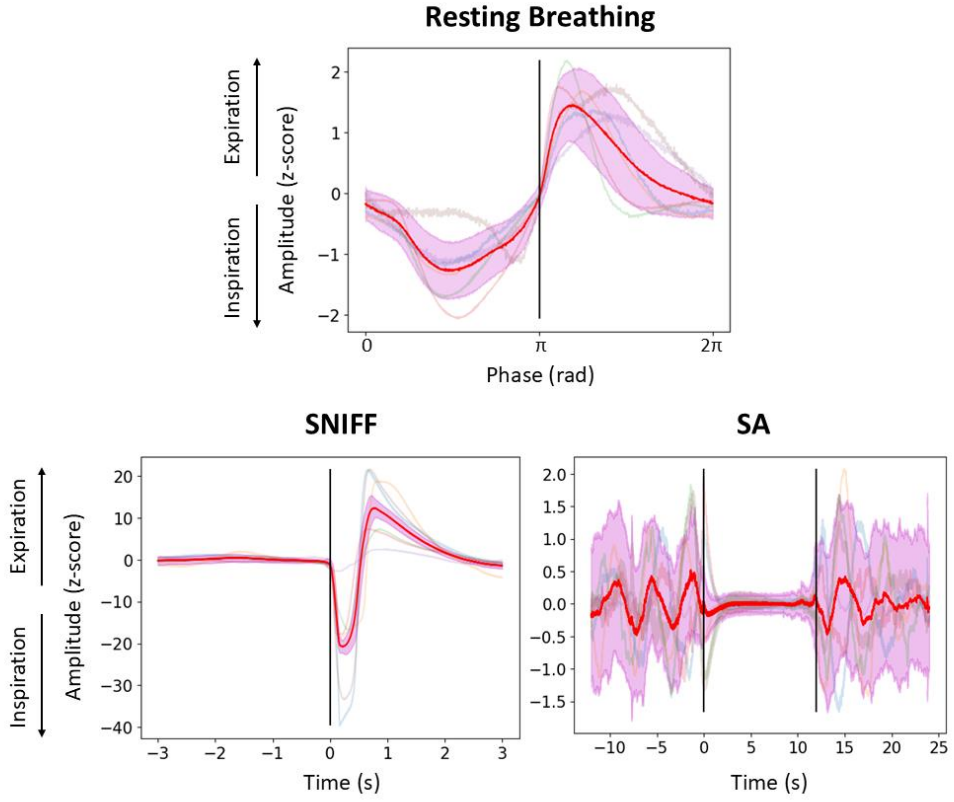

Figure 4. Breathing pattern during resting breathing, sniff manoeuvres (SNIFF) and short apnoeas (SA).
In each panel, the red line depicts the mean nasal pressure time dynamics (expressed in z-score values), with the standard deviation indicated by the pink area. Top panel (resting breathing): superimposed mean respiratory cycles (colored lines representing individual patients; red line representing the population) are relative to the inspiration/expiration transition point (vertical black line). Note that all breathing cycles retained for the resting breathing analysis were normalized to a fixed duration with the objective of eliminating any effect of breath-by-breath individual variability; for this reason, the x-axis of the panel indicates phase rather than time. Bottom left panel (SNIFF): superimposed mean SNIFF manoeuvres (by patient: coloured lines; population: red line) are relative to the start of SNIFF (0). Bottom right panel (short apnoeas, SA): superimposed mean SA cycles (by patient: coloured lines; population: red line) are relative to the start of SA (0).

2. Cortico-limbic power spectrum changes during sniffing

Figure 5A displays the time-frequency maps of the iEEG signal recorded in each ROI. These changes are summarized in the corresponding matrices with the 3 distinct epochs in the abscissa: pre-SNIFF (-1 to 0), SNIFF (0 to 1) and post-SNIFF (1 to 2) (Figure 5B).

During the pre-SNIFF period, there was a significant increase for activities in low frequencies (theta, alpha) power in temporal regions (inferior temporal, medial temporal,

superior temporal gyri), posterior insula gyrus and hippocampus, compared to resting breathing (Figure 5B). This increase covered a larger frequency and time in temporal regions. Simultaneously, a decrease in gamma power was observed in the medial temporal gyrus region.

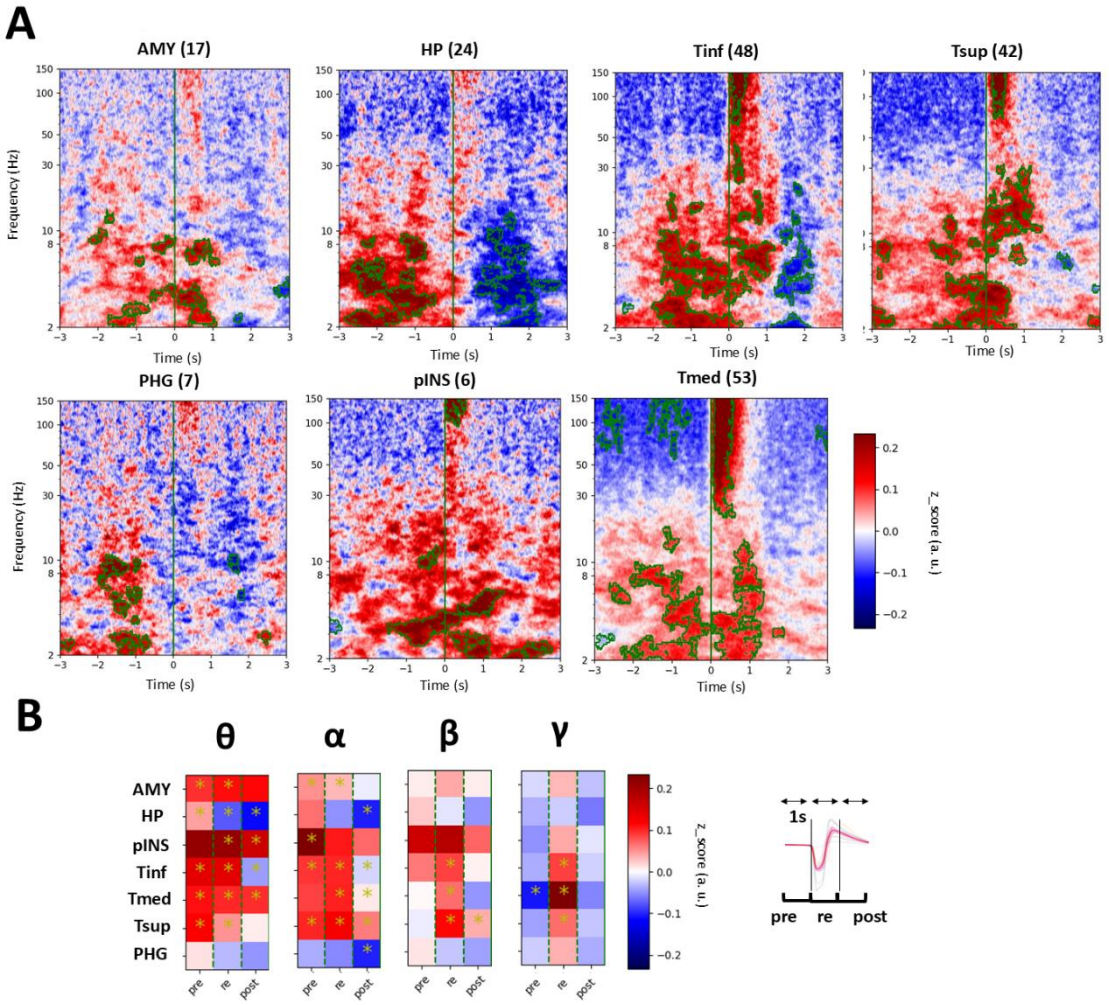

Figure 5. Cortico-limbic dynamics during sniff manoeuvres:
AMY: amygdala; HP, hippocampus; Tinf, inferior temporal gyrus; Tsup, superior temporal gyrus; PHG, parahippocampal gyrus; pINS, posterior insula gyrus; Tmed, medial temporal gyrus.
In panel A, time frequency maps are presented from 3 seconds prior to 3 seconds after the sniff (vertical green line). Power modulations are expressed in terms of zscore differences between resting breathing and sniff results. Statistically significant activity clusters are contoured in green and obtained with a permutation-based approach. Contact numbers for each region are shown in parentheses. **In panel B,** activity is segmented for each frequency band for 1 second during 3 phases, namely the preparation phase ("pre"), the execution phase ("re", for respiratory manoeuvre), and the recovery phase ("post"). In both panels, the dashed green lines mark the transition between preparation and execution ("pre" then "re") and between execution and recovery ("re" then "post"). Significant activity clusters are marked with a yellow star indicating that more than 5% of the segment expressed a significant value under permutation-based cluster.

During the SNIFF period, activities in low frequencies (theta, alpha) power significantly increased in amygdala, inferior temporal, medial temporal, and superior temporal gyri. In addition, a strong increase in gamma power occurred in inferior temporal, superior temporal and medial temporal gyri during the first half of the period. (Figure 5B).

During the post-SNIFF period, activities in low frequencies (theta, alpha) power significantly decreased in hippocampus, parahippocampal gyrus and inferior temporal gyrus (Figure 5B).

3. Cortico-limbic power spectrum changes during short apnoea manoeuvres

Figure 6A displays the time-frequency maps of the iEEG signal recorded in each ROI. These changes are summarised in the corresponding matrices, with the 3 distinct epochs in the abscissa: pre-SA (-12 to 0), SA (0 to 12), post-SA (12 to 24) (Figure 6B).

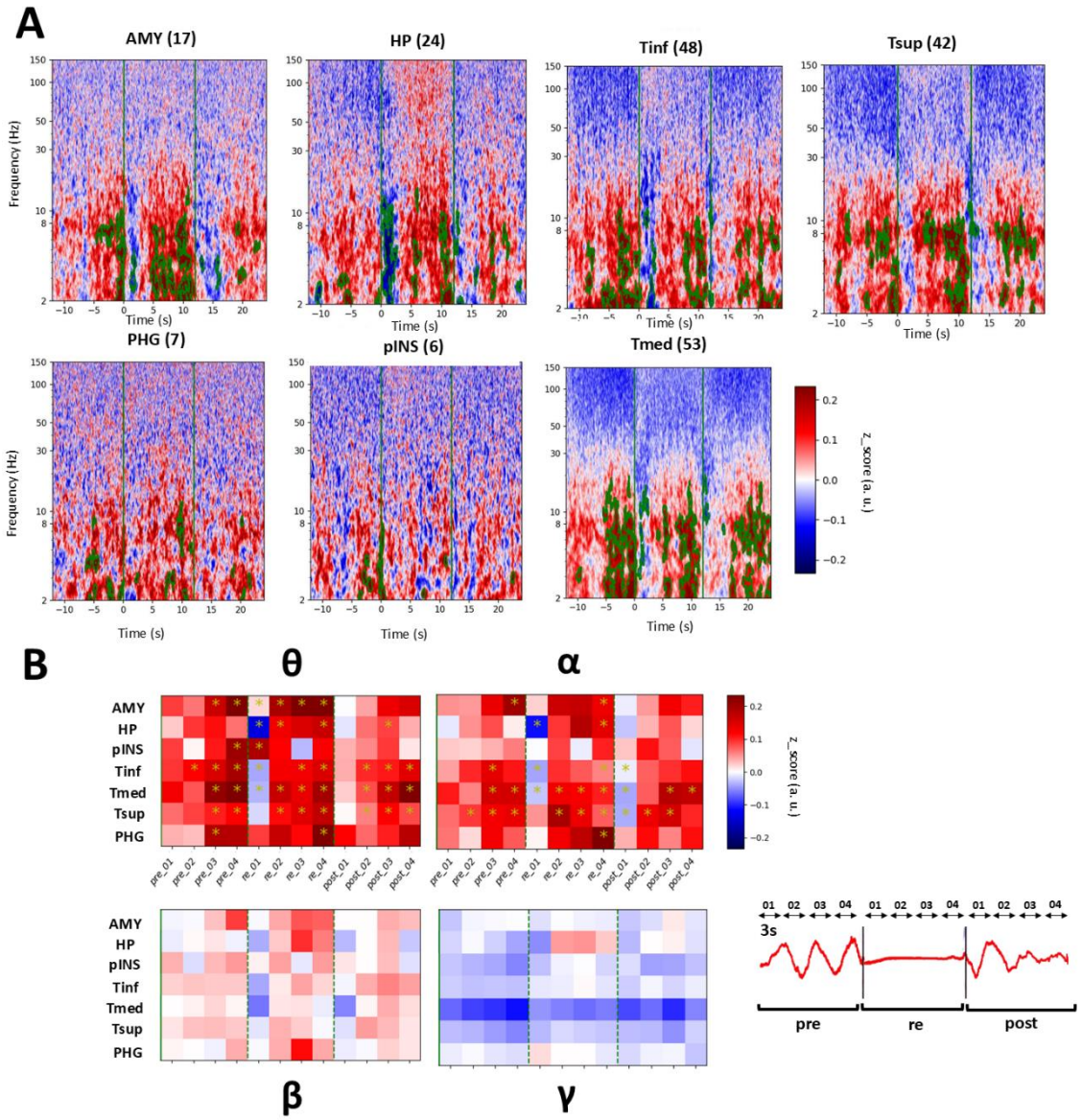

Figure 6. Cortico-limbic dynamics during short apnoeas
AMY: amygdala; HP, hippocampus; Tinf, inferior temporal gyrus; Tsup, superior temporal gyrus; PHG, parahippocampal gyrus; pINS, posterior insula gyrus; Tmed, medial temporal gyrus. **In panel A,** time-frequency maps are presented from 12 seconds before to 24 seconds after the start of the apnoea, shown by the first vertical green line. The second vertical green line shows the end of the apnoea (12 second duration). Power modulations are expressed in terms of standard deviation modulation respective to the resting breathing conditions. Statistically significant activity clusters are contoured in green and obtained with a permutation-based approach. Contact number for each region are shown in

parentheses. **In panel B,** activity is segmented for each frequency band for 3 seconds during 3 phases, namely the preparation phase ("pre"), the execution phase ("re", for respiratory manoeuvre), and the recovery phase ("post"). In both panels, the dashed green lines mark the transition between preparation and execution ("pre" then "re") and between execution and recovery ("re" then "post"). Significant activity clusters are marked with a yellow star indicating that more than 5% of the segment expressed a significant value under permutation-based cluster.

During pre-SA, significant and marked activities in low frequencies (theta, alpha) increases occurred in the temporal region (inferior temporal, medial temporal, superior temporal gyri), amygdala, posterior insula gyrus and parahippocampal gyrus (particularly during the 5 seconds preceding SA).

During SA, significant power modulations were observed in all our ROIs in low frequencies (theta, alpha) in contrast to SNIFF. However, only in amygdala, hippocampus, inferior temporal, medial temporal, and superior temporal gyri, theta and alpha power decreased for the first 3 seconds and then increased until the end of the manoeuvre.

During post-SA, the observed power increases dropped sharply in amygdala, hippocampus, inferior temporal, medial temporal, and superior temporal gyri, and then increased after 3 seconds.

In amygdala, parahippocampal gyrus, hippocampus, inferior temporal, medial temporal, and superior temporal gyri, the increase in theta power observed after the first 3 seconds was statistically significant according to the linear mixed model analysis (Figure 7 and Table 3). This was also the case for the increase in alpha power, except for the superior temporal gyrus (Figure 7B).

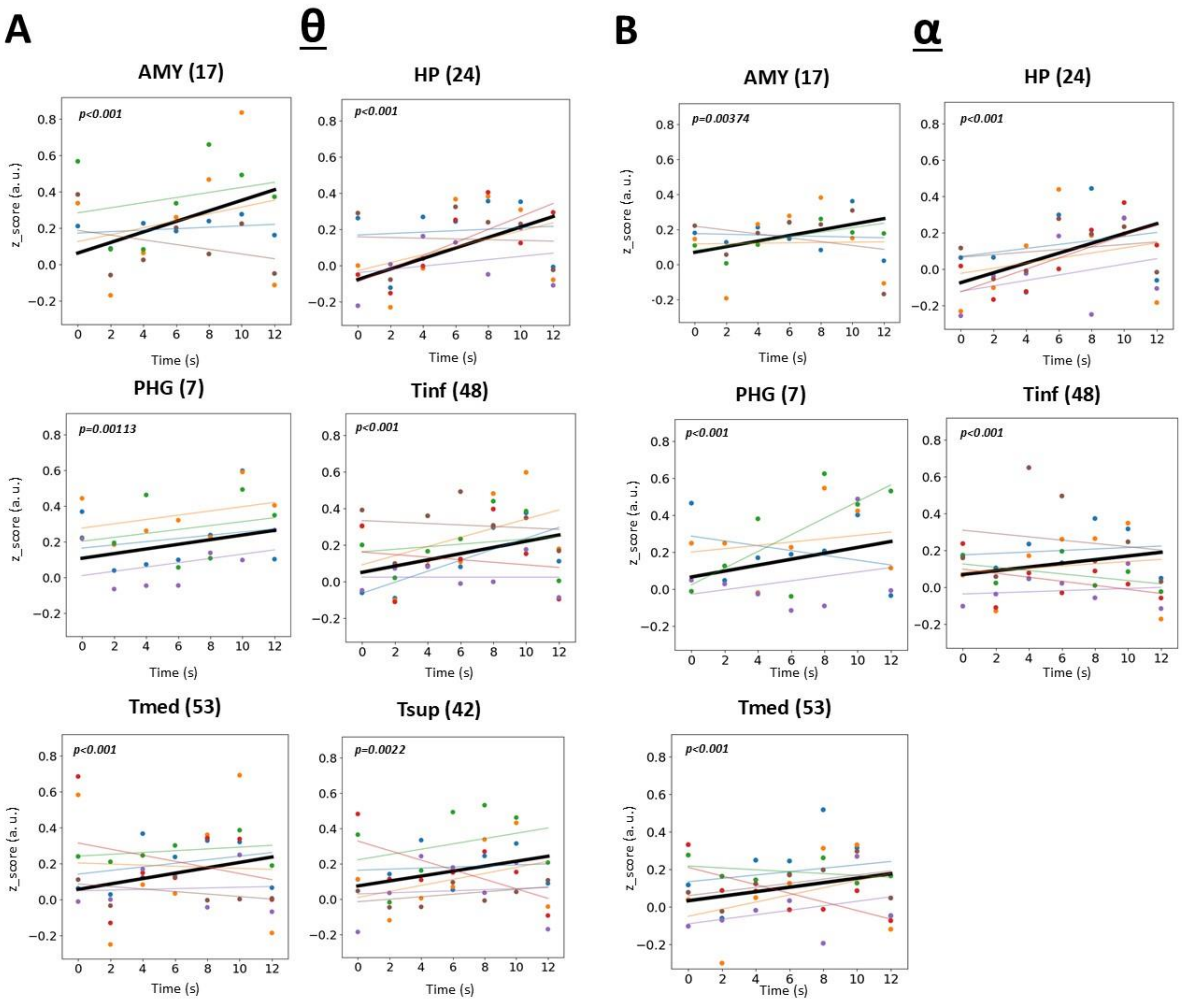

Figure 7. Dynamics of theta and alpha power increase throughout the duration of short apnoeas.
AMY: amygdala; HP, hippocampus; PHG, parahippocampal gyrus; Tinf, inferior temporal gyrus; Tmed, medial temporal gyrus; Tsup, superior temporal gyrus.
Linear mixed model testing power modulations over time for brain regions and band frequencies showing significant power dynamics during SA with patients as a random effect (n=6). For clarity, mean power for 2 second segments are plotted, but p values correspond to the whole signal model. Contact numbers for each region are shown in parentheses. Results are indicated for (**A**) theta band (4-8Hz) and (**B**) for alpha band (8-12Hz).
pvalues are indicated on top left position of each panel (mixed linear model regression)

Figure 8 summarizes the above observations.

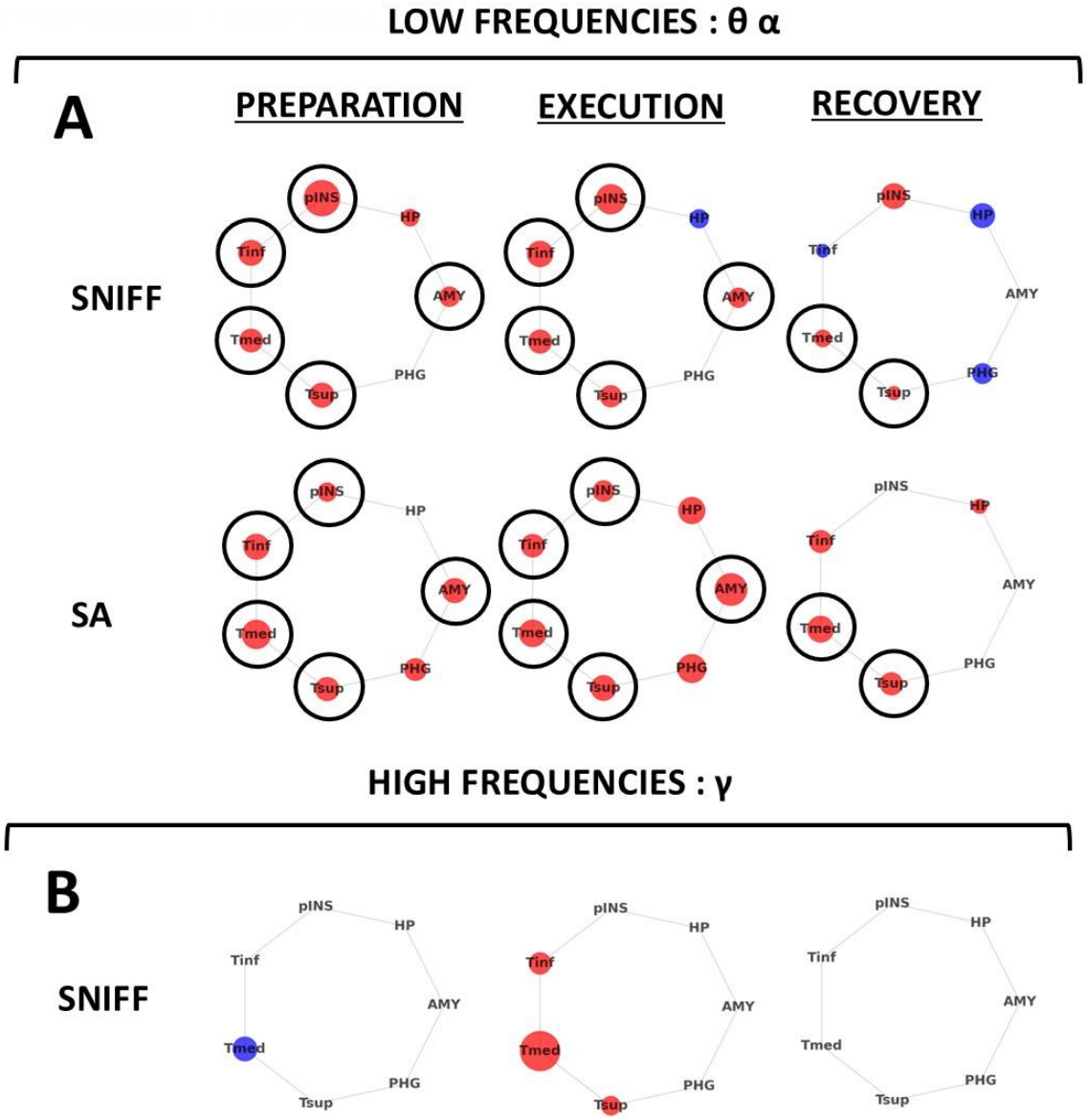

Figure 8. Summary of activity changes in the selected regions of interest during the SNIFF condition and the short apnoea (SA) condition.
In both panels, the seven regions of interest (AMY: amygdala; PHG, parahippocampal gyrus; Tsup, superior temporal gyrus; Tmed, medial temporal gyrus; Tinf, inferior temporal gyrus; pINS, posterior insula gyrus; HP, hippocampus) are represented as the vertices of a heptagon. Coloured dots denote significant changes in power (decrease in blue, increase in red), the size of each dot being proportional to the magnitude of the corresponding change. Black circles indicate regions exhibiting similar power modulation during SNIFF and SA. **Panel A** depicts the observation mades for low frequency bands. **Panel B** depicts the observation made for low frequency bands (SA is not represented because no significant modulation was found).

Discussion

This iEEG study showed that both sniff manoeuvres and SA were associated with oscillatory activity predominantly in low-frequency bands (alpha and theta), with the following specificities: i) the preparation phase of both manoeuvres involved increased alpha and theta activity in the posterior insula, amygdala and temporal regions, with a specific preparatory activity in the parahippocampus for the SA and the hippocampus for sniff; ii) subsequently, it narrowed to

the superior and median temporal areas, immediately after the manoeuvres. During SA, a particular dynamic was observed, consisting of a rapid decline in alpha and theta activity followed by a slow recovery and increase. These observations provide novel insights in the temporal behaviour of part of the networks involved in two respiratory manoeuvres involved in the olfactory control of the environment.

Movement preparation

Like any voluntary movement, the sniff manoeuvre entails cortical preparation. Scalp EEG studies have identified Bereitschaftspotential-like activities followed by motor potentials in central regions, in normal individuals performing repeated sniffs (Macefield and Gandevia, 1991; Raux et al., 2007). These pre-inspiratory potentials occur in the presence of inspiratory loads (Raux et al., 2007) and are associated with breathing discomfort (Georges et al., 2016). Here, we describe sniff preparatory activities involving temporal regions, the posterior insula gyrus, amygdala and hippocampus, indicating that the respiratory-related cortical network mobilised by the preparation of sniff manoeuvres extends beyond premotor and motor regions. Two sniff fMRI studies showed activity in the primary sensorimotor cortex, lateral premotor cortex, supplementary motor area, but also in the cingulate motor area, insula, basal ganglia, thalamus as well as in regions involved in olfactory processing such as the piriform cortex, entorhinal cortex and parahippocampal gyrus (Koritnik et al., 2009; Simonyan et al., 2007). Our observations indicate that some of these fMRI activities, which have previously been interpreted as resulting from afferences or reafferences following motor execution, could also be preparatory in nature.

We also observed iEEG patterns suggestive of preparatory activity before SA. Such a phenomenon has seemingly not been described before using scalp EEG or iEEG. In an fMRI study conducted in 8 healthy volunteers, (McKay et al., 2008) described the neural network responsible for volitional breath-holding during 15-second apnoeas performed from end-expiration (dorsolateral prefrontal cortex and lateral premotor cortex, anterior cingulate cortex, insula, amygdala, basal ganglia, and thalamus). As before, our data indicate that at least part of this network is involved not only in the performance of short voluntary apnoea, but also in their preparation. The activation of the amygdala during the pre-apnoea period is in line with the increasingly established role of the amygdala in breathing inhibition (Dlouhy et al., 2015; Harmata et al., 2023; Nobis et al., 2018; Yang et al., 2020).

The theta power pattern that we observed in the hippocampus is consistent with the hypothesis that unlike other sensory systems, human hippocampal networks are functionally close to the olfactory system. This is based on behavioral results (Chu and Downes, 2002; Plailly et al., 2019) and on iEEG data showing that connectivity between the piriform cortex and hippocampus is modulated by the respiratory cycle in the absence of any olfactory task, especially in the theta frequency band (Zhou et al., 2021). Thus, the SNIFF theta preparatory

activities in the hippocampus could be mediated by a specific exchange with the olfactory system.

Movement execution

Our results show that amygdala, hippocampus, posterior insula gyrus, inferior temporal, medial temporal, and superior temporal gyri are involved during the execution of voluntary sniffs and voluntary apnoeas, in line with available fMRI data (Koritnik et al., 2009; McKay et al., 2008; Simonyan et al., 2007). The particular theta and alpha dynamics that we observed during SA and that was saliently present in the amygdala is consistent with data showing that amygdala activation can provoke apnoea, both in clinical contexts (Dlouhy et al., 2015; Harmata et al., 2023) and experimentally (Nobis et al., 2018), through inhibitory efferent projections to brainstem central pattern generators (Harmata et al., 2023; Liu et al., 2021; Yang et al., 2020). The pattern of SA-related amygdala activation could also correspond to the build-up of an aversive emotion. Animal studies have demonstrated that the amygdala is carbon dioxide sensitive (Ziemann et al., 2009) and that its activation by hypercarbia elicits fear-related behaviour. Given that the apnoea performed by the patients in our study were too short to induce significant carbon dioxide changes, our data suggest that the role of the amygdala during such manoeuvres is more complex than merely a reaction to homeostatic compromise. Having in mind that processing emotionally salient events and successful pattern separation of emotional stimuli in humans engage an amygdala-hippocampus network notably through theta-alpha synchrony (Zheng et al., 2019, 2017), one possibility to interpret our observations would be that activities recorded from the very start of voluntary apnoea are implicated in building a memory trace of an aversive respiratory event. In this context, a recent iEEG study showed theta modulation during fear learning in the amygdala and the medial prefrontal cortex (Chen et al., 2021). Consistent with this hypothesis, the amygdala-hippocampus parallel pattern present during voluntary apnoea was not observed during voluntary sniffs (no hippocampal involvement) that do not carry an aversive background.

We observed a significant increase in gamma power in temporal regions during sniff execution. Surges in gamma activity can be observed during the strong, brisk, and unstoppable muscle contractions that characterise so-called “ballistic" movements. The intensity of gamma oscillations correlates positively with ballistic movement parameters such as velocity, duration, or applied force (Tatti et al., 2023; Ulloa, 2022). Our observations, therefore, provide a neurophysiological substrate to the ballistic nature of sniff manoeuvres. Of note, gamma activities in temporal regions have been described in relationship with speech production and associated movements (Kingyon et al., 2015; Marstaller et al., 2014). Yet speech production requires coordination with respiratory muscles (Fuchs and Rochet-Capellan, 2021), and the dynamics of sniffing resemble those of the sharp inspirations that precede locutory sequences

(prephonatory breaths). It is worth noting that gamma activity measured during sniffing is also seen in regions that typically subserve language.

Methodological considerations

We acknowledge several methodological limitations to the study. First, the small number of patients (n=6) means that caution should be used when interpreting the results. However, recruiting intracranial EEG patients is challenging, and patients must be stringently selected to avoid disease-related biases, cognitive or otherwise, meaning that small numbers of patients are common in iEEG studies (Herrero et al., 2018; Zelano et al., 2016). Second, the recorded brain structures vary across our patients, with a limited number of common electrode locations. This limitation is inherent to iEEG studies because the choice of recorded regions depends on the clinical indication in each patient. In our study, recording activities in the prefrontal cortex and the anterior cingulate gyrus would have been particularly interesting given what is known of suprapontine respiratory-related networks (Evans, 2010; McKay et al., 2008, 2003), and given their implication in both respiratory and olfactory processes (Carlson et al., 2020; Igarashi et al., 2014; Tabert et al., 2007). Also, we did not compare amygdala-hippocampal connectivity between apnoea and sniffs. This type of analysis would have added weight to our data, but posed major difficulties due to the difference in time dynamics between the two conditions. Third, breathing frequency varies across patients, as did the number of manoeuvres performed. This could have biased our results through the introduction of some between-patient variability. Finally, we did not control for the olfactory environment in the patients' bedrooms during the experiment, and olfactory stimuli during the sniffing maneuvers could have interfered with the observation. However, attention to odors is highly important for olfactory consciousness and electrophysiological correlates (Degel and Köster, 1999): when explaining the study to the participants, the possibility that sniffing could induce odor perception was never mentioned, and, naturally, no instruction to pay attention to the olfactory environment was given. Also, there is no reason to think that changes in the olfactory environment in the patients' rooms occurred systematically during the experiments. This environment was most probably generally stable, which must have led to habituation of both the behavioral and neuronal responsiveness (Pellegrino et al., 2017). Of note on this, olfactory changes of usual intensity are very poorly detected (Menzel et al., 2019). In addition to the above, and perhaps most importantly, the permutation analysis that we used contrasts respiratory maneuvers to resting breathing; with this approach, spurious reactions to changes in the olfactory environment cannot statistically contribute to the ERPs observed in response to sniffs.

The study also has strengths. Instead of comparing a period of activity to a pre-event period, which is common in studies of event-related potentials, we performed statistical comparisons between sniffs or apnoeas and resting breathing. This allowed us to study

preparatory activities that would otherwise have been obscured. In addition, we conducted statistical comparisons of sniff and SA data against multiple averaged such segments rather than against single random resting breathing segments, thereby ensuring a more robust threshold of significance. We also used a phase-locked approach rather than a time-locked approach to maximize activity synchronisation and increase the specificity of our statistical threshold.

Putative clinical implications

Olfactory deficits characterize certain diseases altering deep brain structures, like multiple system atrophy or Parkinson's Disease. These deficits, of which the severity relate with disease progression, primarily result from alpha synuclein pathology (Ercoli et al., 2022; Marin et al., 2018). However, sniff execution does determine olfactory performance (Mainland and Sobel, 2006) and olfactory deficits have been linked to sniffing impairment in humans (Sobel et al., 2001). From these observations and our present results, it could be hypothesized that brain rhythms disruptions in limbic structures could contribute to olfactory deficits in these degenerative diseases. This idea aligns with rehabilitation of brain rhythms with deep brain stimulation in Parkinson's Disease having positive impacts on olfactory performances in Parkinson's disease (Brand et al., 2023). A putative link between olfactory deficits and impaired respiratory motor control would justify devising respiratory-targeted therapeutic programs, following a strategy used for motor control in general (Grossauer et al., 2023). Of note, olfactory training can be useful in COVID-19 patients (Pires et al., 2022) and other patients with smell loss (Vance et al., 2023), but the relative contributions of sensory and motor stimulations to these benefits are not known.

Conclusions

This study furthers our understanding of how brain structures involved in producing sniff manoeuvres (Koritnik et al., 2009) and voluntary apnoeas (McKay et al., 2008) interact during the execution of these manoeuvres. In addition, the study is the first to show that limbic structures are involved in their preparation, notably the amygdala and the hippocampus that. appears to play a pivotal role in the orchestration of two respiratory manoeuvres particularly involved in the control of the olfactory environment.

Bibliography

Blomkvist, A., Hofer, M., 2021. Olfactory Impairment and Close Social Relationships. A Narrative Review. Chem Senses 46, bjab037. https://doi.org/10.1093/chemse/bjab037

Bocca, E., Antonelli, A.R., Mosciaro, O., 1965. Mechanical Co-Factors in Olfactory Stimulation. Acta Oto-Laryngologica 59, 243–247. https://doi.org/10.3109/00016486509124558

Brand, G., Bontempi, C., Jacquot, L., 2023. Impact of deep brain stimulation (DBS) on olfaction in Parkinson's disease: Clinical features and functional hypotheses. Revue Neurologique 179. https://doi.org/10.1016/j.neurol.2022.12.013

Carlson, H., Leitão, J., Delplanque, S., Cayeux, I., Sander, D., Vuilleumier, P., 2020. Sustained effects of pleasant and unpleasant smells on resting state brain activity. Cortex 132, 386–403. https://doi.org/10.1016/j.cortex.2020.06.017

Chen, S., Tan, Z., Xia, W., Gomes, C.A., Zhang, X., Zhou, W., Liang, S., Axmacher, N., Wang, L., 2021. Theta oscillations synchronize human medial prefrontal cortex and amygdala during fear learning. Sci Adv 7, eabf4198. https://doi.org/10.1126/sciadv.abf4198

Chu, S., Downes, J.J., 2002. Proust nose best: odors are better cues of autobiographical memory. Mem Cognit 30, 511–518. https://doi.org/10.3758/bf03194952

Colebatch, J.G., Adams, L., Murphy, K., Martin, A.J., Lammertsma, A.A., Tochon-Danguy, H.J., Clark, J.C., Friston, K.J., Guz, A., 1991. Regional cerebral blood flow during volitional breathing in man. J. Physiol. (Lond.) 443, 91–103. https://doi.org/10.1113/jphysiol.1991.sp018824

Degel, J., Köster, E.P., 1999. Odors: implicit memory and performance effects. Chem Senses 24, 317–325. https://doi.org/10.1093/chemse/24.3.317

Desikan, R.S., Ségonne, F., Fischl, B., Quinn, B.T., Dickerson, B.C., Blacker, D., Buckner, R.L., Dale, A.M., Maguire, R.P., Hyman, B.T., Albert, M.S., Killiany, R.J., 2006. An automated labeling system for subdividing the human cerebral cortex on MRI scans into gyral based regions of interest. Neuroimage 31, 968–980. https://doi.org/10.1016/j.neuroimage.2006.01.021

Dlouhy, B.J., Gehlbach, B.K., Kreple, C.J., Kawasaki, H., Oya, H., Buzza, C., Granner, M.A., Welsh, M.J., Howard, M.A., Wemmie, J.A., Richerson, G.B., 2015. Breathing Inhibited When Seizures Spread to the Amygdala and upon Amygdala Stimulation. J Neurosci 35, 10281–10289. https://doi.org/10.1523/JNEUROSCI.0888-15.2015

Ercoli, T., Masala, C., Cadeddu, G., Mascia, M.M., Orofino, G., Gigante, A.F., Solla, P., Defazio, G., Rocchi, L., 2022. Does Olfactory Dysfunction Correlate with Disease Progression in Parkinson's Disease? A Systematic Review of the Current Literature. Brain Sci 12, 513. https://doi.org/10.3390/brainsci12050513

Etkin, A., Egner, T., Kalisch, R., 2011. Emotional processing in anterior cingulate and medial prefrontal cortex. Trends Cogn Sci 15, 85–93. https://doi.org/10.1016/j.tics.2010.11.004

Evans, K.C., 2010. Cortico-limbic circuitry and the airways: insights from functional neuroimaging of respiratory afferents and efferents. Biol Psychol 84, 13–25. https://doi.org/10.1016/j.biopsycho.2010.02.005

Fuchs, S., Rochet-Capellan, A., 2021. The Respiratory Foundations of Spoken Language. Annual Review of Linguistics 7, 13–30. https://doi.org/10.1146/annurev-linguistics-031720-103907

Georges, M., Morawiec, E., Raux, M., Gonzalez-Bermejo, J., Pradat, P.-F., Similowski, T., Morélot-Panzini, C., 2016. Cortical drive to breathe in amyotrophic lateral sclerosis: a dyspnoea-worsening defence? Eur. Respir. J. 47, 1818–1828. https://doi.org/10.1183/13993003.01686-2015

Ghibaudo, V., Granget, J., Dereli, M., Buonviso, N., Garcia, S., 2023. A unifying method to study Respiratory Sinus Arrhythmia dynamics implemented in a new toolbox. https://doi.org/10.31219/osf.io/qbuzy

Grosmaitre, X., Santarelli, L.C., Tan, J., Luo, M., Ma, M., 2007. Dual functions of mammalian olfactory sensory neurons as odor detectors and mechanical sensors. Nat. Neurosci. 10, 348–354. https://doi.org/10.1038/nn1856
Grossauer, A., Sidoroff, V., Heim, B., Seppi, K., 2023. Symptomatic Care in Multiple System Atrophy: State of the Art. Cerebellum 22, 433–446. https://doi.org/10.1007/s12311-022-01411-6
Gu, X., Hof, P.R., Friston, K.J., Fan, J., 2013. Anterior Insular Cortex and Emotional Awareness. J Comp Neurol 521, 3371–3388. https://doi.org/10.1002/cne.23368
Harmata, G.I.S., Rhone, A.E., Kovach, C.K., Kumar, S., Mowla, M.R., Sainju, R.K., Nagahama, Y., Oya, H., Gehlbach, B.K., Ciliberto, M.A., Mueller, R.N., Kawasaki, H., Pattinson, K.T.S., Simonyan, K., Davenport, P.W., Matthew A. Howard, I.I.I., Steinschneider, M., Chan, A.C., Richerson, G.B., Wemmie, J.A., Dlouhy, B.J., 2023. Failure to breathe persists without air hunger or alarm following amygdala seizures. JCI Insight 8. https://doi.org/10.1172/jci.insight.172423
Herrero, J.L., Khuvis, S., Yeagle, E., Cerf, M., Mehta, A.D., 2018. Breathing above the brain stem: volitional control and attentional modulation in humans. J. Neurophysiol. 119, 145–159. https://doi.org/10.1152/jn.00551.2017
Igarashi, M., Ikei, H., Song, C., Miyazaki, Y., 2014. Effects of olfactory stimulation with rose and orange oil on prefrontal cortex activity. Complementary Therapies in Medicine 22, 1027–1031. https://doi.org/10.1016/j.ctim.2014.09.003
Jeran, J., Koritnik, B., Zidar, I., Belič, A., Zidar, J., 2013. Sniffing-related motor cortical potential: topography and possible generators. Respir Physiol Neurobiol 185, 249–256. https://doi.org/10.1016/j.resp.2012.10.006
Jiang, H., Schuele, S., Rosenow, J., Zelano, C., Parvizi, J., Tao, J.X., Wu, S., Gottfried, J.A., 2017. Theta Oscillations Rapidly Convey Odor-Specific Content in Human Piriform Cortex. Neuron 94, 207-219.e4. https://doi.org/10.1016/j.neuron.2017.03.021
Kingyon, J., Behroozmand, R., Kelley, R., Oya, H., Kawasaki, H., Narayanan, N.S., Greenlee, J.D.W., 2015. High-gamma band fronto-temporal coherence as a measure of functional connectivity in speech motor control. Neuroscience 305, 15–25. https://doi.org/10.1016/j.neuroscience.2015.07.069
Koritnik, B., Azam, S., Andrew, C.M., Leigh, P.N., Williams, S.C.R., 2009. Imaging the brain during sniffing: a pilot fMRI study. Pulm Pharmacol Ther 22, 97–101. https://doi.org/10.1016/j.pupt.2008.10.009
Kronland-Martinet, R., J.morlet, Grossmann, A., 2012. Analysis of sound patterns through wavelet transforms. International Journal of Pattern Recognition and Artificial Intelligence 01. https://doi.org/10.1142/S0218001487000205
Kulason, S., Ratnanather, J.T., Miller, M.I., Kamath, V., Hua, J., Yang, K., Ma, M., Ishizuka, K., Sawa, A., 2022. A comparative neuroimaging perspective of olfaction and higher-order olfactory processing: on health and disease. Semin Cell Dev Biol 129, 22–30. https://doi.org/10.1016/j.semcdb.2021.08.009
Liu, J., Hu, T., Zhang, M.-Q., Xu, C.-Y., Yuan, M.-Y., Li, R.-X., 2021. Differential efferent projections of GABAergic neurons in the basolateral and central nucleus of amygdala in mice. Neurosci Lett 745, 135621. https://doi.org/10.1016/j.neulet.2020.135621
Macefield, G., Gandevia, S.C., 1991. The cortical drive to human respiratory muscles in the awake state assessed by premotor cerebral potentials. J. Physiol. (Lond.) 439, 545–558. https://doi.org/10.1113/jphysiol.1991.sp018681
Mainland, J., Sobel, N., 2006. The sniff is part of the olfactory percept. Chem. Senses 31, 181–196. https://doi.org/10.1093/chemse/bjj012
Marin, C., Vilas, D., Langdon, C., Alobid, I., López-Chacón, M., Haehner, A., Hummel, T., Mullol, J., 2018. Olfactory Dysfunction in Neurodegenerative Diseases. Curr Allergy Asthma Rep 18, 42. https://doi.org/10.1007/s11882-018-0796-4
Maris, E., Oostenveld, R., 2007. Nonparametric statistical testing of EEG- and MEG-data. J Neurosci Methods 164, 177–190. https://doi.org/10.1016/j.jneumeth.2007.03.024
Marstaller, L., Burianová, H., Sowman, P.F., 2014. High Gamma Oscillations in Medial Temporal Lobe during Overt Production of Speech and Gestures. PLOS ONE 9, e111473. https://doi.org/10.1371/journal.pone.0111473

McKay, L.C., Adams, L., Frackowiak, R.S.J., Corfield, D.R., 2008. A bilateral cortico-bulbar network associated with breath holding in humans, determined by functional magnetic resonance imaging. Neuroimage 40, 1824–1832. https://doi.org/10.1016/j.neuroimage.2008.01.058

McKay, L.C., Evans, K.C., Frackowiak, R.S.J., Corfield, D.R., 2003. Neural correlates of voluntary breathing in humans. J. Appl. Physiol. 95, 1170–1178. https://doi.org/10.1152/japplphysiol.00641.2002

Menzel, S., Hummel, T., Schäfer, L., Hummel, C., Croy, I., 2019. Olfactory change detection. Biol Psychol 140, 75–80. https://doi.org/10.1016/j.biopsycho.2018.11.010

Nobis, W.P., Schuele, S., Templer, J.W., Zhou, G., Lane, G., Rosenow, J.M., Zelano, C., 2018. Amygdala-stimulation-induced apnea is attention and nasal-breathing dependent. Ann. Neurol. 83, 460–471. https://doi.org/10.1002/ana.25178

Pellegrino, R., Sinding, C., de Wijk, R.A., Hummel, T., 2017. Habituation and adaptation to odors in humans. Physiology & Behavior 177, 13–19. https://doi.org/10.1016/j.physbeh.2017.04.006

Pérez-García, F., Lehongre, K., Bardinet, E., Jannin, P., Navarro, V., Hasboun, D., Fernandez-Vidal, S., 2015. Automatic Segmentation Of Depth Electrodes Implanted In Epileptic Patients: A Modular Tool Adaptable To Multicentric Protocols. Epilepsia 56, 227.

Phelps, E.A., LeDoux, J.E., 2005. Contributions of the amygdala to emotion processing: from animal models to human behavior. Neuron 48, 175–187. https://doi.org/10.1016/j.neuron.2005.09.025

Physiology of Breath-Hold Diving and the Ama of Japan: Papers, 1965. . National Academies Press, Washington, D.C. https://doi.org/10.17226/18843

Pires, Í. de A.T., Steffens, S.T., Mocelin, A.G., Shibukawa, D.E., Leahy, L., Saito, F.L., Amadeu, N.T., Lopes, N.M.D., Garcia, E.C.D., Albanese, M.L., De Mari, L.F., Ferreira, I.M., Veiga, C.A., Jebahi, Y., Coifman, H., Fornazieri, M.A., Hamerschmidt, R., 2022. Intensive Olfactory Training in Post-COVID-19 Patients: A Multicenter Randomized Clinical Trial. Am J Rhinol Allergy 36, 780–787. https://doi.org/10.1177/19458924221113124

Plailly, J., Villalba, M., Vallat, R., Nicolas, A., Ruby, P., 2019. Incorporation of fragmented visuo-olfactory episodic memory into dreams and its association with memory performance. Sci Rep 9, 15687. https://doi.org/10.1038/s41598-019-51497-y

Raux, M., Straus, C., Redolfi, S., Morelot-Panzini, C., Couturier, A., Hug, F., Similowski, T., 2007. Electroencephalographic evidence for pre-motor cortex activation during inspiratory loading in humans. J. Physiol. (Lond.) 578, 569–578. https://doi.org/10.1113/jphysiol.2006.120246

Roberts, S.C., Havlíček, J., Schaal, B., 2020. Human olfactory communication: current challenges and future prospects. Philos Trans R Soc Lond B Biol Sci 375, 20190258. https://doi.org/10.1098/rstb.2019.0258

Schottelkotte, K.M., Crone, S.A., 2022. Forebrain control of breathing: Anatomy and potential functions. Front Neurol 13, 1041887. https://doi.org/10.3389/fneur.2022.1041887

Sharma, A., Kumar, R., Aier, I., Semwal, R., Tyagi, P., Varadwaj, P., 2019. Sense of Smell: Structural, Functional, Mechanistic Advancements and Challenges in Human Olfactory Research. Curr Neuropharmacol 17, 891–911. https://doi.org/10.2174/1570159X17666181206095626

Simonyan, K., Saad, Z.S., Loucks, T.M.J., Poletto, C.J., Ludlow, C.L., 2007. Functional neuroanatomy of human voluntary cough and sniff production. Neuroimage 37, 401–409. https://doi.org/10.1016/j.neuroimage.2007.05.021

Sobel, N., Thomason, M.E., Stappen, I., Tanner, C.M., Tetrud, J.W., Bower, J.M., Sullivan, E.V., Gabrieli, J.D., 2001. An impairment in sniffing contributes to the olfactory impairment in Parkinson's disease. Proc Natl Acad Sci U S A 98, 4154–4159. https://doi.org/10.1073/pnas.071061598

Tabert, M.H., Steffener, J., Albers, M.W., Kern, D.W., Michael, M., Tang, H., Brown, T.R., Devanand, D.P., 2007. Validation and optimization of statistical approaches for modeling odorant-induced fMRI signal changes in olfactory-related brain areas. Neuroimage 34, 1375–1390. https://doi.org/10.1016/j.neuroimage.2006.11.020

Tatti, E., Cacciola, A., Carrara, F., Luciani, A., Quartarone, A., Ghilardi, M.F., 2023. Movement-related ERS and connectivity in the gamma frequency decrease with practice. NeuroImage 284, 120444. https://doi.org/10.1016/j.neuroimage.2023.120444

Thomas-Danguin, T., Sinding, C., Romagny, S., El Mountassir, F., Atanasova, B., Le Berre, E., Le Bon, A.-M., Coureaud, G., 2014. The perception of odor objects in everyday life: a review on the processing of odor mixtures. Frontiers in Psychology 5.

Ulloa, J.L., 2022. The Control of Movements via Motor Gamma Oscillations. Front. Hum. Neurosci. 15. https://doi.org/10.3389/fnhum.2021.787157

Vance, D.E., Del Bene, V.A., Kamath, V., Frank, J.S., Billings, R., Cho, D.-Y., Byun, J.Y., Jacob, A., Anderson, J.N., Visscher, K., Triebel, K., Martin, K.M., Li, W., Puga, F., Fazeli, P.L., 2023. Does Olfactory Training Improve Brain Function and Cognition? A Systematic Review. Neuropsychol Rev 1–37. https://doi.org/10.1007/s11065-022-09573-0

Yang, C.F., Kim, E.J., Callaway, E.M., Feldman, J.L., 2020. Monosynaptic Projections to Excitatory and Inhibitory preBötzinger Complex Neurons. Front Neuroanat 14, 58. https://doi.org/10.3389/fnana.2020.00058

Yang, Q., Zhou, G., Noto, T., Templer, J.W., Schuele, S.U., Rosenow, J.M., Lane, G., Zelano, C., 2022. Smell-induced gamma oscillations in human olfactory cortex are required for accurate perception of odor identity. PLoS Biol 20, e3001509. https://doi.org/10.1371/journal.pbio.3001509

Yeshurun, Y., Sobel, N., 2010. An odor is not worth a thousand words: from multidimensional odors to unidimensional odor objects. Annu Rev Psychol 61, 219–241, C1-5. https://doi.org/10.1146/annurev.psych.60.110707.163639

Zelano, C., Jiang, H., Zhou, G., Arora, N., Schuele, S., Rosenow, J., Gottfried, J.A., 2016. Nasal Respiration Entrains Human Limbic Oscillations and Modulates Cognitive Function. J. Neurosci. 36, 12448–12467. https://doi.org/10.1523/JNEUROSCI.2586-16.2016

Zheng, J., Anderson, K.L., Leal, S.L., Shestyuk, A., Gulsen, G., Mnatsakanyan, L., Vadera, S., Hsu, F.P.K., Yassa, M.A., Knight, R.T., Lin, J.J., 2017. Amygdala-hippocampal dynamics during salient information processing. Nat Commun 8, 14413. https://doi.org/10.1038/ncomms14413

Zheng, J., Stevenson, R.F., Mander, B.A., Mnatsakanyan, L., Hsu, F.P.K., Vadera, S., Knight, R.T., Yassa, M.A., Lin, J.J., 2019. Multiplexing of Theta and Alpha Rhythms in the Amygdala-Hippocampal Circuit Supports Pattern Separation of Emotional Information. Neuron 102, 887-898.e5. https://doi.org/10.1016/j.neuron.2019.03.025

Zhou, G., Olofsson, J.K., Koubeissi, M.Z., Menelaou, G., Rosenow, J., Schuele, S.U., Xu, P., Voss, J.L., Lane, G., Zelano, C., 2021. Human hippocampal connectivity is stronger in olfaction than other sensory systems. Prog Neurobiol 201, 102027. https://doi.org/10.1016/j.pneurobio.2021.102027

Ziemann, A.E., Allen, J.E., Dahdaleh, N.S., Drebot, I.I., Coryell, M.W., Wunsch, A.M., Lynch, C.M., Faraci, F.M., Howard, M.A., Welsh, M.J., Wemmie, J.A., 2009. The amygdala is a chemosensor that detects carbon dioxide and acidosis to elicit fear behavior. Cell 139, 1012–1021. https://doi.org/10.1016/j.cell.2009.10.029

Additional information

FUNDING

Jules Granget was supported by a doctoral fellowship from *Institut Universitaire d'Ingénierie en Santé (IUIS),* Sorbonne Université, Paris, France and by the French National Research Agency (ANR-22-CE37-0014, BreathSmellRelax)

AUTHOR CONTRIBUTIONS J.G., M.C.N., N.B., T.S. conceived and designed research; J.G., M.C.N., K.L. performed experiments; J.G., K.L. analyzed data; J.G., M.C.N., K.L., V.N., N.B., T.S. interpreted results of experiments; J.G. prepared figures; J.G., M.C.N., N.B., T.S., drafted manuscript; J.G., M.C.N., K.L., V.L., V.F., V.N., N.B., T.S. edited and revised manuscript; J.G., M.C.N., K.L., V.L., V.F., V.N., N.B., T.S. approved final version of manuscript.

DATA AVAILABILITY STATEMENT

All of the individual participant data collected during the experiments and duly deidentified will be made available immediately following publication, with no end date, to researchers who provide a methodologically sound proposal having been approved by an independent review committee ("learned intermediary") identified for this purpose. Data requests should be directed to the corresponding author (thomas.similowski@sorbonne-universite.fr), noting that to gain access, data requestors will need to sign a data access agreement.

The Python scripts used in this study, including for iEEG pre-processing and processing pipeline and statistics, are all available at the following URL:

https://github.com/JulesGranget/Script_Python_iEEG_Paris_git

Tables

Table 1. Clinical information

patient	age	sex	handedness	presumed epileptic zone (according to scalp EEG)	baseline antiepileptic medication
1	27	M	Right	temporal pole	Brivacetam, Carbamazepine
2	29	F	Right	hippocampal regions of the two sides	Zonisamide, Carbamazepine
3	38	M	Right	temporal pole, amygdala	Lamictal
4	33	F	Left	left hippoampus	Lamotrigine, Brivacetam
5	44	F	Right	temporal pole, amygdala	Oxcarbazepine, Lacosamide, Zonisamide, Porpanolol
6	26	M	Right	temporal pole, anterior temporo basal regions	Perampanel, Eslicarbazepine

Table 2. Number of respiratory events used for iEEG analysis

Participant	Resting Breathing	SNIFF	SA
1	65	49	34
2	89	58	36
3	56	91	26
4	67	29	24
5	113	73	39
6	53	66	39

Table 3. Linear mixed model coefficient for time-dependent power modification in SA.

Frequency Band	ROI	Fixed effect Coefficients*	Z-values**	P-value
Alpha	amygdala	0.016	3.718	0.00374
Alpha	hippocampus	0.027	-2.322	p<0.001
Alpha	inferior temporal gyrus	0.01	1.868	p<0.001
Alpha	medial temporal gyrus	0.012	1.039	p<0.001
Alpha	superior temporal gyrus	0.004	4.697	0.37
Alpha	parahippocampal gyrus	0.016	1.448	p<0.001
Alpha	posterior insula	0.011	1.317	0.935
Theta	amygdala	0.029	1.429	p<0.001
Theta	hippocampus	0.029	-1.811	p<0.001
Theta	inferior temporal gyrus	0.017	1.72	p<0.001
Theta	medial temporal gyrus	0.015	1.686	p<0.001
Theta	superior temporal gyrus	0.014	1.68	0.0022
Theta	parahippocampal gyrus	0.013	1.744	0.00113
Theta	posterior insula	0.001	4.13	0.992

* represent the average relationship across the entire population and depend on the strength and direction of the relationship between the predictor variables and the outcome, adjusted for fixed and random effects; ** calculated by dividing the coefficient estimate by its standard error (SE), they provide an estimation of effect size (the higher Z, the greater the effect size).